A Density Functional Theory Study of Molecular and Dissociative Adsorption of H_2 on Active Sites in Mordenite

L. Benco,*,†,‡ T. Bucko,† J. Hafner,† and H. Toulhoat§

Institut für Materialphysik and Center for Computational Materials Science, Universität Wien, Sensengasse 8, A-1090 Wien, Austria, Institute of Inorganic Chemistry, Slovak Academy of Sciences, Dubravska cesta 9, SK-84236 Bratislava, Slovak Republic, and Institut Français du Pétrole, F-92852 Rueil-Malmaison Cedex, France

Received: June 22, 2005; In Final Form: September 13, 2005

Adsorption and chemisorption of H_2 in mordenite is studied using ab initio density functional throry (DFT) calculations. The geometries of the adsorption complex, the adsorption energies, stretching frequencies, and the capacity to dissociate the adsorbed molecule are compared for different active sites. The active centers include a Brønsted acid site, a three-coordinated surface Al site, and Lewis sites formed by extraframework cations: Na^+, Cu^+, Ag^+, Zn^{2+}, Cu^{2+}, Ga^{3+}, and Al^{3+}. Adsorption properties of cations are compared for a location of the cation in the five-membered ring. This location differs from the location in the six-membered ring observed for hydrated cations. The five-membered ring, however, represents a stable location of the bare cation. In this position any cation exhibits higher reactivity compared with the location in the six-membered ring and is well accessible by molecules adsorbed in the main channel of the zeolite. Calculated adsorption energies range from 4 to 87 kJ/mol, depending on electronegativity and ionic radius of the cation and the stability of the cation−zeolite complex. The largest adsorption energy is observed for Cu^+ and the lowest for Al^{3+} integrated into the interstitial site of the zeolite framework. A linear dependence is observed between the stretching frequency and the bond length of the adsorbed H_2 molecule. The capacity of the metal-exchanged zeolite to dissociate the H_2 molecule does not correlate with the adsorption energy. Dissociation is not possible on single Cu^+ cation. The best performance is observed for the Ga^{3+}, Zn^{2+}, and Al^{3+} extraframework cations, in good agreement with experimental data.

1. Introduction

Zeolites are used in many industrial processes as catalysts, ion exchangers, molecular sieves, and carriers.[1] The catalytic activity of zeolites is driven by active sites that are always present in zeolite structures. Usually any perturbation of the siliceous framework behaves as an active site. Zeolite structures can contain a variety of active sites differing in character and concentration. Typical representatives are Brønsted and Lewis acid sites (BAS and LAS) with a proton or an extraframework cation compensating the charge on the framework created by an Al/Si substitution.

The importance of the BAS for intrazeolite conversion processes is demonstrated by a reaction rate increasing with the concentration of acid sites. BAS play a role in proton-exchange processes. A comparison of the adsorption strength of different types of acid sites shows that BAS belong to weak adsorption sites.[2] The acid proton easily attacks basic molecules, like NH_3. An attack of the acid proton on stable molecules, such as saturated hydrocarbons, requires a high activation energy of ∼100 to ∼220 kJ/mol[3] and therefore is possible only at high temperatures.[4]

The strongest adsorption centers in zeolites are LAS. Lewis sites exhibit the largest adsorption energies,[2] and molecules adsorbed on LAS show the largest frequency shifts of the molecular stretching modes upon the adsorption.[5] LAS in zeolites are either extraframework cations compensating framework Al/Si substitutions or microaggregates of oxo-species. Locations and activities of extraframework cations vary with the degree of coordination. Hydrated cations are fully coordinated by water molecules. Upon dehydration a coordination by solvent is replaced with incomplete coordination by framework O-atoms. Consequently, cations move closer to the framework and exhibit increasing adsorption power and reactivity. In the reduction atmosphere extraframework cations can be reduced and form metal particles. The negatively charged porous zeolite framework even allows the stabilization of unusual oxidation states, such as Zn^+.[6,7]

Among a large variety of intrazeolite oxo-species of particular importance are aluminum oxides (extraframework aluminum, EFAl). The state of aluminum in EFAl particles produced by the dealumination of Y zeolite was reported by Jiao et al.[8] Gola et al.[9] have identified and quantified EFAl particles in stabilized Y zeolite. An investigation of the nature of EFAl species in zeolite USY has been reported by Omegna et al.[10,11] The relation between framework and extraframework Al and the catalytic performance of Pt/USY catalysts was studied by Arribas and Martinez.[12] They found that the concentration of EFAl relates to the total acidity of the catalyst which determines the product yield and selectivity of the conversion. The EFAl particles thus seem to play an important role in the intrazeolite chemistry. The concentration of EFAl depends on conditions of the zeolite manufacturing and can be modified by drastic chemical or

* Corresponding author. Tel: +43-1-4277-51407. Fax: + 43-1-4277-9413. E-mail: lubomir.benco@univie.ac.at.

† Institut für Materialphysik and Center for Computational Materials Science, Universität Wien.

‡ Institute of Inorganic Chemistry, Slovak Academy of Sciences.

§ Institut Français du Pétrole.

10.1021/jp0533729 CCC: $30.25
Published on Web 11/04/2005

hydrothermal treatment like acid leaching and steaming.[5] Al atoms are extracted from the zeolite framework and increase the concentration of extraframework LAS. EFAl particles formed by Al atoms released from the framework are difficult to characterize. Little is known about their precise composition, the coordination of the Al atoms, and the bonding between particle and framework. The extraframework particles bind to Al/Si substitutions that survived the dealumination of the framework. Because Al/Si substitutions and extraframework particles are distributed randomly, diffraction techniques cannot be used for their characterization. Other techniques, like NMR, provide only averaged information. Another difficulty originates from the low concentration of the most active sites. Despite frequent statements underlining the importance of LAS in determining the reactivity of zeolites, the role of Lewis centers in catalytic processes remains largely unclear.

In our recent work we investigate various forms of EFAl particles including hydrated aluminum oxo-species[13] and bare Al^{3+} cations deposited on the inner surface of the zeolite.[2] We suggest that Al^{3+} can exist as a bare cation fixed in a rigid part of the zeolite framework.[2] A series of C−O stretching bands measured for CO adsorbed in zeolites compares reasonably well with frequencies calculated for CO adsorbed on active sites. The C−O stretching band at ∼2230 cm^{-1} [5] exhibiting a huge blue shift, in particular, can be explained only as resulting from CO adsorbed on a site as strong as a bare Al^{3+} cation locally stabilized on the zeolite framework.[2] A relation between stability and reactivity of a Lewis site in the zeolite was recently constructed for Zn-exchanged mordenite.[14] We demonstrate that global stability of the Zn-exchanged zeolite is governed by the distribution of framework Al/Si substitutions. In low-Al zeolites the extraframework cation is located close to the isolated framework Al site. A complete analysis of all locations of the framework Al site and the extraframework Zn^{2+} cation shows that the most stable location of the cation is in a six-membered ring (6MR) in agreement with experimental data.[15] Depending on the position of the framework Al site, the Zn^{2+} cation deposited in the five-membered ring (5MR) can represent a locally stable configuration. Moreover, the Zn^{2+} cation on the 5MR with Al/Si substitution in the T4 site represents a local configuration supporting the dissociative adsorption of H_2 and CH_4.[14]

In the present work we extend the study of Brønsted and Lewis sites investigated recently[2,14] by a large series of bare extraframework cations. The set of Lewis sites now includes Al ions both in extraframework positions and in interstitial sites. We compare extraframework Al sites with three-coordinated Al at the surface of the zeolite and with a series of bare extraframework cations, Na^+, Cu^+, Ag^+, Cu^{2+}, Zn^{2+}, Ga^{3+}, and Al^{3+}, deposited on the 5MR. Although no clear experimental evidence for this location of the cation exists, we investigate adsorption properties of this configuration because it represents a reaction pathway for the dissociative adsorption of small molecules[14] and therefore could be at a low concentration crucial for the catalytic performance of the zeolite. We use a periodic DFT method to characterize the properties of active sites via the strength of H_2 adsorption. The degree of activation of the H_2 molecule induced by molecular adsorption is discussed as a function of the charge, electronegativity, and ionic radius of different extraframework cations. We evaluate adsorption geometries and energies for both molecular and dissociative adsorption. Finally, we use the recently developed concept of the intrazeolite reaction pathway[14] to assess the capacity of extraframework cations to dissociate a H_2 molecule.

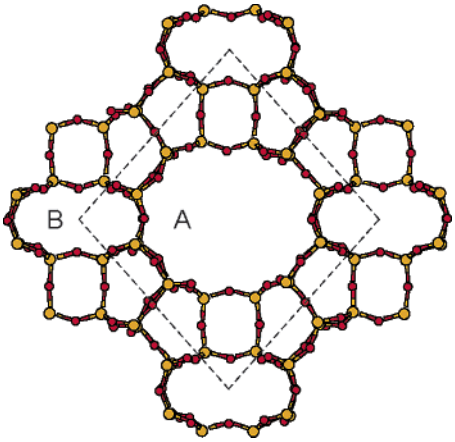

Figure 1. Structure of mordenite projected along the *c* axis. The largest channels are the 12-membered ring (A) and the 8-membered side channel (B). Dotted lines indicate the monoclinic unit cell.

2. Structure and Computational Setup

Structure and Active Sites. Our investigations have been performed on mordenite. Mordenite belongs to the zeolites used most frequently in industrial catalysis, it has been used in many fundamental studies devoted to the chemical reactivity of zeolites. The calculations use the monoclinic unit cell of mordenite optimized for the purely siliceous structure[16] with dimensions $a = b = 13.675$ Å, $c = 7.540$ Å. The structure of mordenite is displayed in Figure 1. The monoclinic cell was previously used for simulations of the adsorption of CO[2] and NH_3[17] and for the investigation of properties of Zn^{2+} Lewis sites.[14] Prior to Al/Si substitutions, the cell contains 72 atoms, 24 tetrahedral Si sites, and 48 O sites. Al/Si substitutions in T sites of the mordenite framework balancing the charge of the extraframework mono-, bi-, and trivalent cations, respectively, produce structures with a Si/Al ratio of 23, 11, and 7, typical for low-Al zeolites.

Active sites for which the adsorption of H_2 is compared are displayed in Figure 2; some of them are the same as previously used for the adsorption of CO.[2] Among many possible locations of BAS, we have chosen those with the acid protons oriented into the zeolite main channel (see Figure 2a). An extraframework aluminum (EFAl) was previously investigated experimentally[8−12] and theoretically.[13,18] In the present work we consider EFAl in two different configurations formed upon the deposition of the Al^{3+} cation on a flexible and on a rigid part of the framework. A flexible part is the six-membered ring (6MR) allowing penetration of the cation into the interstitial position. Depending on the local concentration of Al/Si substitutions in the framework, two different configurations can be formed in the 6MR. At high concentration the extraframework cation moves into the interstitial site surrounded by three framework Al sites (see Figure 2b). Because this configuration is stable and electronically well balanced, no reconstruction of the framework occurs. Note, however, that in this position the Al^{3+} cation can make only loose contact with molecules adsorbed in the main channel (Figure 2b). In a low-Al zeolite the charge of the extraframework Al^{3+} cation is compensated with Al/Si substitutions located in the framework at large distances. When deposited on a flexible part of the framework the Al^{3+} cation causes a local reconstruction of the bonding forming a small amorphous-like particle (not displayed in Figure 2). More details on the local reconstruction of the framework are given in our recent work.[2] No reconstruction occurs when a cation is deposited on a rigid part of the framework, such as the 5MR (see Figure 2c). A cation

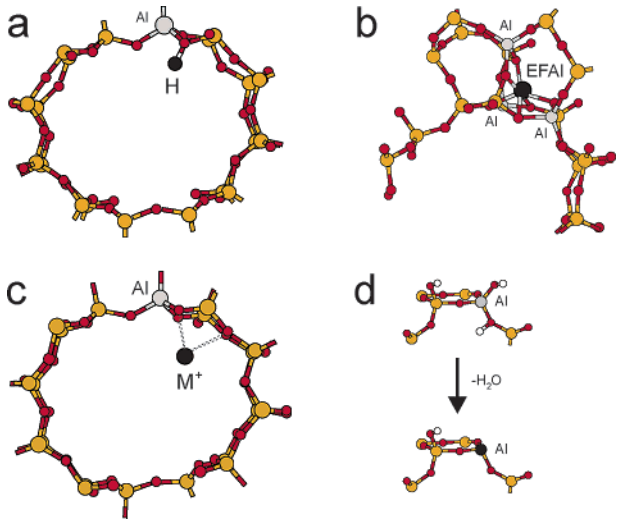

Figure 2. Active sites in mordenite (full circles). Brønsted acid proton (a) compensating one framework Al/Si substitution. Extraframework aluminum deposited in the 6MR representing a flexible part of the framework (b). The Al^{3+} cation moves into an interstitial site and compensates three Al/Si substitutions. Extraframework cation deposited in the 5MR representing a rigid part of the framework (c). The cation remains located in the main channel. Three-coordinated Al atom (d) formed via the dehydration of the surface removing one surface silanol group and the acid proton.

deposited on the 5MR remains located in the main channel. In this position the extraframework cation represents an active site available for interactions with adsorbates. In our recent work we observe that Al^{3+} and Zn^{2+} cations deposited on the 5MR exhibit considerable adsorption strength. Such Lewis sites are strong enough to break bonds of adsorbed molecules.[2,14] A very stable location of the extraframework cation found in mordenite is in the 6MR,[14] in good agreement with experimental observations.[15] The location in the 5MR is not observed experimentally. Cations located in the 5MR exhibit much higher activity than those located in the 6MR.[14] It is therefore likely that despite low occupancy the sites above the 5MR are crucial for intrazeolite conversion processes. In this work we compare adsorption and chemisorption of H_2 on active sites in mordenite with adsorption on a series of cations (Na^+, Cu^+, Ag^+, Cu^{2+}, Zn^{2+}, Ga^{3+}, Al^{3+}) located in the 5MR (see Figure 2c). Finally, adsorption properties of a three-coordinated surface Al atom are probed as well. This surface perturbation is formed via the dehydration of surface sites saturated by terminal silanol groups (Figure 2d).[19] At extremely high temperatures, a fraction of three-coordinated Al atoms increases to 5−10% of all mordenite T sites.[20]

In our recent work on adsorption of H_2 and CH_4 on Zn-MOR, we observe that dissociation is supported by such a local configuration that has a capacity to locally stabilize the proton.[14] Figure 3 compares two local configurations with the extraframework cation on the 5MR but with different location of the Al/Si substitution. In low-Al mordenite containing isolated Al/Si substitutions, the effective reaction pathway exists only for the configuration containing Al in the T4 site (see Figure 3a). In this configuration the proton abstracted from the adsorbed molecule connects to the O atom of the 4MR, where it is well stabilized. On the other hand a configuration with Al in the T2 site (see Figure 3b) does not support deprotonation, because of the poor capacity of the Al−O−Si bond to accommodate the proton. In the present work we investigate adsorption properties of a series of the extraframework cations constituting the local structure that supports the dissociative adsorption. For the Al^{3+}

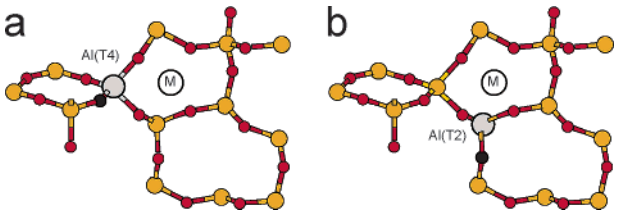

Figure 3. Local configuration with the extraframework cation deposited on the 5MR. Al in T4 site supports deprotonation of adsorbed molecules and represents effective reaction pathway (a). Al in T2 site does not support deprotonation (b). M is the extraframework cation and the black circle is a proton-accepting O site.

cation, however, both configurations representing the reaction path (RP) and the nonreaction path (NRP) are compared.

Throughout the text the following notation for the extraframework cation is used: $M^{x+}(y)$ stands for a x-valent extraframework cation deposited on the 5MR containing y Al/Si framework substitutions. $Cu^{2+}(1)$ thus represents an extraframework Cu^{2+} cation in mordenite with two compensating framework Al/Si substitutions located at a large distance, one of which is in the 5MR. The Cu^{2+} cation resides close to one Al/Si substitution such as to bind to as many framework O atoms as possible.

Simulation Technique. The periodic density functional theory (DFT) calculations are performed using the Vienna Ab initio Simulation Package (VASP).[21−24] The Kohn−Sham equations are solved using the local exchange-correlation functional by Perdew and Zunger[25] corrected for nonlocality according to Perdew et al. (PW91).[26] Ultrasoft pseudopotentials[27,28] and a plane-wave basis set are used as implemented in the VASP package.[24] The calculations are performed using Blöchl's projector augmented wave technique[29,30] with a plane-wave cutoff energy of 400 eV. Because of the large unit cell, Brillouin-zone sampling is restricted to the Γ point.[31] Convergence is improved using a modest smearing of the eigenvalues. Gaussian-like partial occupancies of energy levels are introduced around the Fermi level, and the total energy is extrapolated to the zero smearing. The relaxation of structures is performed via a conjugate-gradient algorithm until differences of the total energies are converged below 10^{-5} eV per cell. To calculate IR spectra, fixed-volume molecular dynamics simulations are performed at 20 K. The dynamics uses the exact Hellmann−Feynman forces acting on atoms and applies the statistics of the canonical ensemble to the motion of atomic nuclei[32] and the Verlet velocity algorithm[33] with a time step for the integration of equations of motion of $\Delta t = 1.0$ fs. The frequency of the heat bath is fixed to the frequency of the Si−O stretching of the zeolite framework. The simulation time is 4 ps. The frequency spectra are calculated via Fourier transform of the velocity autocorrelation function.

3. Results

3.1. Molecular Adsorption. Geometries. The H_2 molecule interacts with an active site via the bonding electron density accumulated between the two H atoms. The adsorption therefore leads to a flat configuration with the molecule oriented approximately parallel to the inner surface of the zeolite. Two typical adsorption complexes showing the adsorption on a Brønsted acid site and on an extraframework cation are displayed in Figure 4. The adsorption geometry is characterized by three main parameters. For a BAS these are the bond length r_1 of the acidic hydroxyl group, the distance r_2 between the

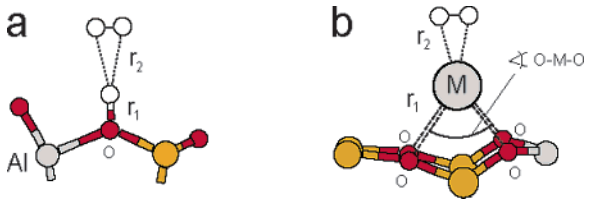

Figure 4. Geometry of the H_2 molecule adsorbed on the Brønsted acid site (a) and on the extraframework Lewis site (b). The extraframework cation is deposited on the 5MR of the zeolite framework.

TABLE 1: Geometry of the Adsorption Complex of H_2 on Different Active Sites[a]

site	r_1	r_2	H−H	O−M−O
BAS[b]	0.983	1.910	0.755	
Na^+	2.414	2.555	0.754	102, 105
$Cu^{2+}(2)$	1.972	2.426	0.757	151, 154
$Al^{3+}(3)$[c]	1.989	∼4.3	0.751	140, 151, 171
$Al^{3+}(1)$rec[d]	1.833	2.324	0.759	162, 164
Al-3c[e]	1.695	2.174	0.761	118, 120, 121
$Al^{3+}(2)$	1.812	2.059	0.770	153, 162
$Al^{3+}(1)$RP[f]	1.826	2.005	0.776	150, 154
$Al^{3+}(1)$NRP[g]	1.829	2.002	0.777	147, 147
$Zn^{2+}(2)$	1.955	1.969	0.776	115, 115
$Zn^{2+}(1)$	2.067	1.927	0.780	127, 133
$Ga^{3+}(1)$	1.935	2.030	0.784	140, 145
$Cu^{2+}(1)$	2.144	1.739	0.801	121, 128
$Ag^+(1)$	2.399	1.874	0.804	90, 93
$Cu^+(1)$	2.075	1.588	0.857	70, 78

[a] Cations are placed in the 5MR and 6MR of the mordenite framework. Distances in Å and angles in deg. [b] BAS = Brønsted acid site (cf. Figure 2a). [c] The extraframework Al^{3+} cation is completely integrated into the framework and makes contact with six O atoms. The coordination sphere is a deformed AlO_6 octahedron. All six O atoms are neighbors to the framework Al atoms. No local reconstruction of the framework occurs (see Figure 2b). [d] $Al^{3+}(1)$rec is the Al^{3+} cation accommodated in the 6MR. The cation is incorporated in the framework causing a local reconstruction of the structure (not displayed in Figure 2). [e] Al-3c is a framework Al site formed upon dehydration of the zeolite surface (see Figure 2d). [f] RP represents the extraframework Al^{3+} cation deposited on one framework Al/Si substitution in the 5MR constituting a reaction path (cf. Figure 3a and ref 14). [g] NRP = nonreaction path (see Figure 3b).

proton and the H atoms of the adsorbed molecule, and the H−H bond length. For a LAS the geometry is described by the average cation−oxygen distance r_1, the O−M−O angle, the distance between the cation and the adsorbate, and the H−H bond length (Figure 4). Geometry parameters of adsorption complexes formed on different active sites are collected in Table 1.

The correlation between the distance of the cation from the framework and the distance of the adsorbed H_2 molecule from the cation is displayed in Figure 5. The M−O distance, denoted as r_1 (Figure 4b), is averaged over the shortest contacts to the O atoms of the framework. Most of the cations are deposited on a 5MR and form four contacts to the O atoms of the framework (Figure 4b). A slightly different configuration is observed for the most electronegative atoms Ag and Cu. Their cations are also located in the 5MR, but in an asymmetric position considerably shifted toward the framework Al atom and interacting with just two O atoms. Of a different character are the sites Al-3c and $Al^{3+}(1)$rec. The former is a three-coordinated defect site formed on the surface upon the dehydration of terminal silanol groups (see Figure 2d).[19] In contrast to the other cations this site is not an extraframework site but represents a perturbation of the framework. The second site is the product of the local reconstruction of the framework which occurs upon deposition of an extraframework Al^{3+} cation in the 6MR of the zeolite main channel containing just one Al/Si

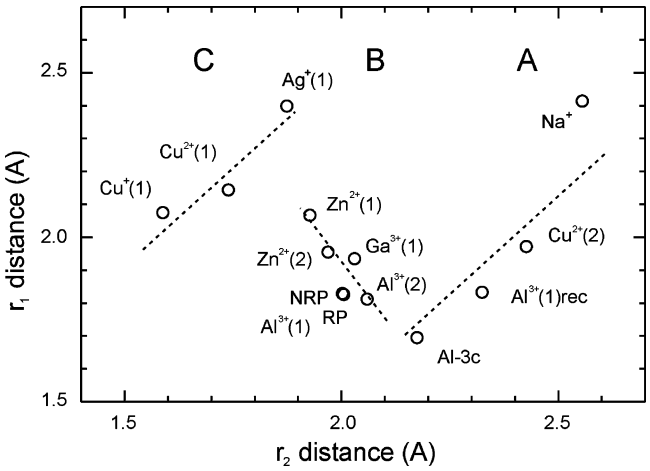

Figure 5. Correlation between average cation−oxygen distance r_1 and adsorbate−cation distance r_2. Dashed lines are guides to the eye, suggesting the existence of three different categories of active sites (A, B, C).

framework substitution. In the flexible 6MR the undercoordinated extraframework cation integrates into the structure and forms an irregular AlO_x polyhedron;[2] see also Figure 2b.

The distance r_1 of the extraframework cation from the framework O atoms ranges from ∼1.8 Å ($Al^{3+}(2)$, $Al^{3+}(1)$rec) to ∼2.4 Å (Ag^+, Na^+). This distance depends on the charge of the cation, the ionic radius, and the number of contacts to charge-compensating Al/Si substitutions, and reflects the strength of the cation-to-zeolite interaction. The shorter the distance, the stronger is the bonding between the cation and the zeolite framework. Cation binding is the loosest for the monovalent cations Ag^+, Na^+, and Cu^+. Bonding of intermediate strength is observed for Cu^{2+}, Zn^{2+}, and Ga^{3+}. For polyvalent cations, the closeness to more than one charge-compensating Al/Si site leads to a shorter M−O distance, i.e., to stronger binding. The most strongly bound are the extraframework Al^{3+} cations. The Al-3c site is a framework site, and the distance r_1 1.695 Å corresponds to the Al−O bond length. The bonding of this atom is trigonal and planar with O−Al−O angles close to 120° (cf. Table 1).

The distance of the H_2 molecule from the cation ranges from 1.6 Å (Cu^+) to 2.6 Å (Na^+). The dashed lines outlined in Figure 5 indicate the correlation between the bonding of the cation to the framework (r_1) and the distance between the cation and the adsorbate (r_2) for three different categories of active sites. The sites keeping the adsorbed molecule at a large distance include the bulky Na^+ cation, the framework perturbation Al-3c, and the $Cu^{2+}(2)$ and the $Al^{3+}(1)$rec cations (group A, see Figure 5). The first two belong to weak adsorption centers (cf. below). In the $Al^{3+}(1)$rec configuration the cation is incorporated into the skeleton of the zeolite where it causes a local reconstruction of the framework. The $Cu^{2+}(2)$ cation is deposited on a 5MR comprising two Al/Si substitutions. Upon the contact with two framework Al sites, the divalent Cu^{2+} cation is pulled out of the main channel of the zeolite into the plane of the 5MR. Both Cu^{2+} and Al^{3+} extraframework cations are hidden in the framework, forming large O−M−O angles (cf. Table 1). Because of the tight contact with the O atoms of the framework, the charge of these two cations is rather compensated and the cations exhibit rather low activity. The distance between the adsorbed molecule and the active site is therefore large. The dashed line indicates that within group A of Lewis sites the adsorbate distance r_2 changes proportionally with the oxygen−cation distance r_1 (see Figure 5).

TABLE 2: Changes in the Average Cation−Oxygen Distance Induced by the Adsorption of H_2 (in Å)

cation	r_1 (before adsorption)	r_1 (after adsorption)	Δr_1 (%)	no. of M−O contacts
$Al^{3+}(2)$	1.811	1.825	0.77	4
$Zn^{2+}(1)$	2.034	2.067	1.60	4
$Cu^{2+}(1)$	2.048	2.144	4.48	4
$Cu^{+}(1)$	1.985	2.075	4.34	2

The second group of adsorption complexes (B) includes the polyvalent cations Al^{3+}, Ga^{3+}, and Zn^{2+} placed in a small 5MR of the framework. Because of the limited flexibility of the small ring, the cations remain on the inner surface of the zeolite without any local reconstruction of the framework. The configurations formed by polyvalent cations are less stable than the well-balanced $Cu^{2+}(2)$ and $Al^{3+}(1)$rec structures and, therefore, exhibit higher reactivity.[14] Interestingly, within group B the distance r_2 of the H_2 molecule from the active site increases (i.e., the adsorption strength decreases, cf. the following subsection) as the metal−oxygen distance r_1 decreases demonstrating a tighter binding of the cation to the framework.

The third group of Lewis sites (C) comprises extraframework noble-metal atoms that attract the H_2 molecule to a short distance ranging from 1.6 to 1.9 Å. The reason for the strong binding is the rather high electronegativity of the extraframework atom (1.90 and 1.93 for Cu and Ag, respectively[34]). The larger value of r_2 observed for the Ag^+ cation is in accordance with the larger ionic radius of this cation (74 and 114 pm for tetracoordinated Cu^+ and Ag^+, respectively[34]). Interestingly, the Cu^{2+} cation with a smaller ionic radius (71 pm compared with 74 pm of the Cu^+ cation) is located at a larger distance from the framework. The reason for this apparent anomaly becomes clear if we consider the geometry of the Cu−MOR complex. Both cations are deposited on the 5MR with one Al/Si substitution. The Cu^{2+} cation establishes four contacts with O atoms of the 5MR with an averaged distance of 2.144 Å (Table 1). Distances of all four contacts are of similar length, and the extraframework cation resides in a quasi-symmetrical 5MR site. The bulkier Cu^+ cation interacts only with two O atoms of the framework, and therefore two Cu−O distances are shorter than those of the Cu^{2+} cation. The reconstruction of the Cu−MOR complex leading to a decreased number of contacts with the framework and to the less symmetrical position of the extraframework cation makes the Cu^+ cation more unsaturated. Hence the Cu^+ cation attracts the H_2 molecule to a shorter distance than Cu^{2+}.

The interaction of the H_2 molecule with the cation induces a slight change of the position of the extraframework cation relative the zeolite surface. The bare cation is attracted to the O atoms of the zeolite more strongly than after adsorption of the H_2 molecule. Table 2 lists the M−O distances of selected cations before and after adsorption of H_2. For all cations an increase of the distance between the cation and the framework is observed. The change of the distance, however, is a function of both the strength of the interaction between the cation and the zeolite and the strength of the interaction between H_2 and the cation. The smallest change of the M−O distance of 0.77% occurs for the $Al^{3+}(2)$ site. This demonstrates a very strong interaction between the Al^{3+} cation and the framework and rather weak interaction of H_2 with the cation. A slightly larger change is observed for the $Zn^{2+}(1)$ site and the largest change occurs for the Cu^{2+} and the Cu^+ cations. For both Cu sites the metal−oxygen distance increases by ∼4.40%. The similar pull-out, however, results from a combination of two different effects. For Cu^{2+} we have a relatively weak interaction with four framework oxygens and a weak cation−adsorbate interaction. Cu^+ is bound more strongly to only two oxygens and binds also more strongly to the H_2 molecule.

TABLE 3: Adsorption Energies, Bond Lengths of the Adsorbed H_2 Molecule, and Dissociation Energies on Different Active Sites[a]

site	E_{ads}	r_{H-H}	E_{diss}[b]
free H_2		0.750	
BAS	16.5	0.755	*c*
$Na^+(1)$	12.6	0.754	*c*
$Cu^{2+}(2)$	11.0	0.757	+12.0
$Al^{3+}(3)$	3.5	0.751	+66.1
$Al^{3+}(1)$rec	13.1	0.759	+37.0
Al-3c	15.3	0.761	+38.0
$Al^{3+}(2)$	36.7	0.769	−63.5
$Al^{3+}(1)$RP	57.9	0.776	−99.0
$Al^{3+}(1)$NRP	57.8	0.777	−69.8
$Zn^{2+}(2)$	31.3	0.776	−20.3
$Zn^{2+}(1)$	55.1	0.780	−61.1
$Ga^{3+}(1)$	35.6	0.784	−188.7
$Cu^{2+}(1)$	45.6	0.801	−5.1
$Ag^+(1)$	62.8	0.804	+72.0
$Cu^+(1)$	86.5	0.857	+70.0

[a] Energies in kJ/mol and distances in Å. Notation of sites as in Table 1. [b] $E_{diss} < 0$ indicates the ability of the active site to dissociate the H_2 molecule. The dissociation energy is calculated as a difference between the total energy of products accommodated in the zeolite and the total energy of the site with adsorbed nondissociated molecule. [c] On Na^+ and BAS the dissociation products convert to the neutral H_2 molecule.

Adsorption Energies. The calculated adsorption energies are listed in Table 3 together with the H−H bond lengths of the adsorbed molecule and the dissociation energies of the H_2 molecule. According to the adsorption energies, the active sites are distinguished in three groups: weak sites (0−20 kJ/mol), sites with the intermediate adsorption strength (30−60 kJ/mol), and strong sites (60−90 kJ/mol). The first group includes the Brønsted acid site, the perturbed surface Al site (Al-3c), the Na^+ extraframework cation with low electronegativity, and "strong" higher valency extraframework cations stabilized via tight contacts with the framework ($Al^{3+}(3)$, $Al^{3+}(1)$rec, $Cu^{2+}(2)$). As pointed out above, for these sites the adsorbate−cation distance r_2 increases with the cation−oxygen distance; here we find that the adsorption energy decreases with increasing r_2.

Upon adsorption electron density is transferred from the interatomic region of the H_2 molecule to the active site of the zeolite. A depletion of the bonding electron density makes the H−H bond weaker and leads to an increase of the bond length. The correlation between the adsorption energy and the H−H distance of the adsorbed molecule is displayed in Figure 6. Because of the different character of the active sites, different valencies, ionic radii, oxidation states, and electronegativities of extraframework cations, the points of the correlation are considerably scattered. The weakly adsorbing sites of group A lead only to a very modest activation of the H_2 molecule. A much more pronounced elongation of the H−H bond length is observed for the stronger adsorption on sites of types B and C.

The adsorption energy is inversely proportional to the stability of the site. The relation between stability and reactivity was recently demonstrated for the adsorption of H_2 on Zn−MOR structures.[14] The more tightly the extraframework cation binds to the zeolite framework, the lower is the adsorption strength of the cation. The stabilizing cation-to-zeolite interaction critically depends on the number of framework Al/Si substitutions in direct contact with the extraframework cation. The most stable configuration is formed when the number of the Al atoms in the framework in close proximity of the cation equals the valency of the cation. E.g., the $Al^{3+}(3)$ site represents an

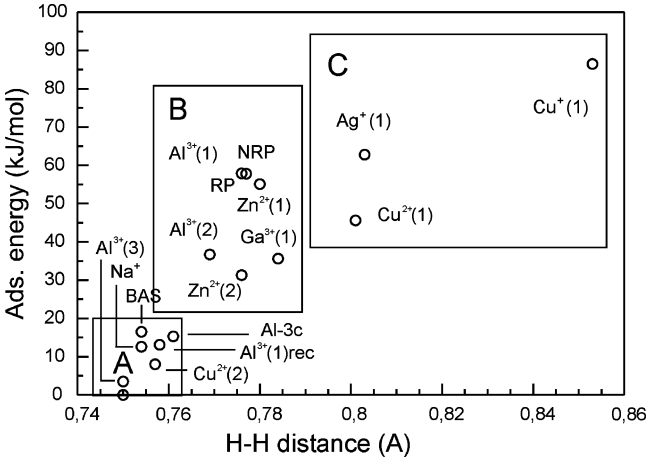

Figure 6. Adsorption energies of H_2 on different Lewis sites. Frames are a guide to the eye outlined for different electronegativities of the extraframework atoms.

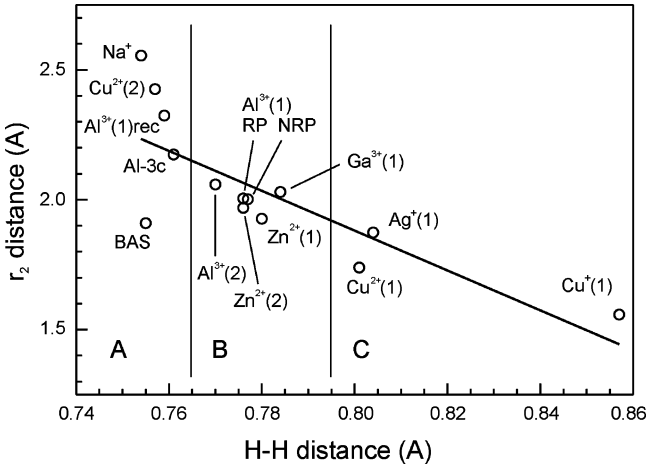

Figure 7. Bond activation of the adsorbed H_2 molecule. The r_2 parameter represents the averaged distance between the H atoms and the cation (cf. Figure 4). The full line is the least-squares fit.

extraframework Al^{3+} cation fully integrated into the zeolite framework (cf. Table 1). Because of the contact with three Al/Si framework substitutions, the site is very stable. The calculated adsorption energy of 3.5 kJ/mol demonstrates an extremely low adsorption strength of the site. In the $Al^{3+}(2)$ site the extraframework Al^{3+} cation interacts with only two Al/Si framework substitutions. In such a position the charge of the extraframework cation is not completely balanced and the separation of charges between cation and zeolite framework is much larger than that for the $Al^{3+}(3)$ site. The adsorption energy calculated for $Al^{3+}(2)$ increases to 36.7 kJ/mol. The increase of the adsorption energy correlates to a much lower stability compared with the $Al^{3+}(3)$ site. When the extraframework Al^{3+} cation is located in the vicinity of just one framework Al/Si substitution (as could be the case in a low-Al zeolite), the adsorption energy increases to ~58 kJ/mol. The high adsorption energy correlates to a low stability of the site resulting from the large separation of charges between the extraframework Al^{3+} cation and the zeolite framework.

A similar correlation between the stability of the active sites and their adsorption strength is apparent for Zn−MOR and Cu−MOR (cf. Table 3 and Figure 6). The more stable $Zn^{2+}(2)$ site exhibits a lower adsorption energy of 31.3 kJ/mol than the less stable $Zn^{2+}(1)$ site with 55.1 kJ/mol. Note, however, that the $Zn^{2+}(2)$ site still exhibits considerable reactivity. The Zn^{2+} cation deposited on two framework Al/Si substitutions retains a high adsorption capacity because it does not penetrate the structure and remains on the inner zeolite surface. Because of the asymmetry of the environment of the cation, the positive charge of the cation and the negative charge of the framework oxygens remain separated and such an extraframework Zn^{2+} cation exhibits a high adsorption strength and high reactivity.

The adsorption energy of H_2 on extraframework Cu cations is high both for the $Cu^{+}(1)$ and for the $Cu^{2+}(1)$ sites (86.5 and 45.6 kJ/mol, respectively). For the $Cu^{2+}(2)$ site the adsorption energy decreases to 11 kJ/mol. The reason for the radical reduction of the adsorption strength is the reconstruction of bonding leading to the incorporation of the Cu^{2+} cation into the 5MR. Because of the tight binding between the cation and the O atoms of the framework, the cation is strongly screened, leading to a considerable decrease of the adsorption strength. A catalytic activity of bivalent Cu^{2+} cations could be therefore expected only for zeolites with low concentration of Al forming $Cu^{2+}(1)$ active sites. Considerably higher, however, is the activity of the $Cu^{+}(1)$ site. Among the compared extraframework cations, Cu^{+} exhibits the largest adsorption strength (Table 3 and Figure 6). As already discussed above the reason behind the increased activity of this site is the different structure of the Cu^{+}−MOR complex. The weaker bonding to the framework allows a shift of the extraframework cation toward the O atoms bound to the framework Al atom. The shift results in the asymmetric position of Cu^{+} within the 5MR in which only two Cu−O contacts are established. Such a Cu^{+}−MOR complex is considerably less stable than the Cu^{2+}−MOR site, and the Cu^{+} cation exhibits higher adsorption strength than Cu^{2+}.

The valency of the cation influences the adsorption energy as well. With increased valency of the extraframework cation, a strengthening of the interaction between the cation and the framework occurs. The increased strength of the interaction leads to the formation of more stable structures and therefore to the decrease of the adsorption energy. The adsorption energy of the $Cu^{+}(1)$ site is 86.5 kJ/mol. The two-valent cation Cu^{2+} deposited on the same site of the framework forms the more stable structure with the adsorption energy decreased to 45.6 kJ/mol.

Activation of H_2. The increase of the bond length of H_2 induced by the adsorption on the active site in the zeolite represents an activation of the adsorbed molecule. As already discussed above, the activation is correlated to the adsorption energy (cf. Figure 6). For the extraframework cations the adsorption energy is a complex function of both the interaction between the molecule and the cation and between the cation and the zeolite framework. The correlation between the bond length of H_2 and the distance r_2 of the molecule from the active site is displayed in Figure 7. The degree of the activation increases with decreasing r_2. In analogy with the r_1/r_2 correlation displayed in Figure 5 the adsorption sites can be classified in three different groups denoted as A, B, and C.

Only a small degree of bond activation is observed for sites in group A. The group includes the weakest adsorption centers with adsorption energies smaller than 20 kJ/mol (cf. Figure 6). Upon adsorption on these centers the bond length of H_2 increases from 0.750 Å to a value not larger than 0.765 Å. Distances of the molecule from the active center are widely scattered. The large r_2 distance for Na^{+} is due to the large ionic radius of the cation. In contrast, the short r_2 distance for the BAS corresponds to the small diameter of the proton. Large distances of H_2 are observed also for extraframework cations integrated into the zeolite framework such as $Cu^{2+}(2)$ and $Al^{3+}(1)$rec because of the location of the cation deep in the framework of the zeolite.

TABLE 4: Stretching Frequencies *f* of the H_2 Molecule for Different Active Sites[a]

site	H−H distance[b]	*f*[c]	Δ*f*(free H_2)	Δ*f*(BAS)-calc	Δ*f*(BAS)-exp
free H_2	0.750 (0.751)	4384[d] (4161)		+101	+61
Al^{3+}(3)	0.751	4365	−19	+82	
Na^{+}(1)	0.754	4307	−77	+24	∼+20[e]
BAS	0.755	4283 (4100)	−101		
Cu^{2+}(2)	0.757	4252	−132	−31	
Al^{3+}(1)rec	0.759	4216	−168	−67	−72
Al-3c	0.761	4185	−199	−98	
Al^{3+}(2)	0.769	4066	−318	−217	
Al^{3+}(1)RP	0.776	3993	−391	−290	
Al^{3+}(1)NRP	0.777	3978	−406	−305	
Zn^{2+}(2)	0.776	3971	−413	−312	
Zn^{2+}(1)	0.780	3914	−470	−369	
Ga^{3+}(1)	0.784	3629	−755	−654	
Cu^{2+}(1)	0.801	3583	−801	−700	
Ag^{+}(1)	0.804	3539	−845	−744	∼−800[f]
Cu^{+}(1)	0.857	2913	−1471	−1370	−805, −980, −1030[g]

[a] Two shifts Δ*f* are calculated relative to the frequency of the free H_2 molecule and relative to H_2 adsorbed on the BAS. Distances in Å and frequencies in cm^{-1}. Notation of sites as In Table 1. [b] Bond length is averaged over all configurations of the MD run (in parentheses experimental distance). [c] Stretching frequency is calculated as Fourier transform of the velocity autocorrelation function (in parentheses experimental frequency). [d] Stretching frequency of the free molecule is calculated as the average of two rotational-vibration (P and R) branches of the diatomic molecule. [e] ZSM-5 (ref 36). [f] Reference 38. [g] Reference 39.

Such a cation is no longer an exposed active site, and the adsorbed molecule feels not only the attraction by the cation but also the repulsion by the framework. Because of this repulsion, the capacity of the cations to adsorb molecules is considerably reduced.

Group B consists of the "strong" cations Zn^{2+}, Al^{3+}, and Ga^{3+} deposited on the inner surface of the zeolite. These cations form less stable structures exhibiting high adsorption capacity and activity. The adsorption energies of these sites range from 30 to 60 kJ/mol (cf. Table 3). They attract the H_2 molecule to distances ranging from 2.059 Å (Al^{3+}(2)) to 1.927 Å (Zn^{2+}(1)) and increase the bond length of H_2 to 0.775 Å and 0.785 Å.

The largest bond activation is observed for the extraframework atoms Ag and Cu (group C). The Ag^{+} and Cu^{+} cations are only weakly bound to the framework; the distance of the cation from the framework oxygens is as large as that for the Na^{+} cation (cf. Figure 5). The distance r_2 between the cation and the adsorbed molecule is reduced to 1.874 Å for Ag^{+} and to 1.739 Å for Cu^{+}. The largest activation of H_2 observed for Cu^{+} is reflected by an extension of the bond length by 14%. The Cu^{2+} cation deposited on one Al/Si substitution in the framework forms a structure that is more stable than the Cu^{+}-(1) site, but Figure 7 shows that the Cu^{2+}(1) site still belongs to the most activating zeolite sites.

Stretching Frequencies. The bond activation of the adsorbed H_2 molecule leads to the downshift of the intramolecular stretching frequency. The frequencies deduced via Fourier transform of the velocity autocorrelation function calculated from a molecular dynamics simulation are listed in Table 4 and plotted in Figure 8 against the H−H bond length. The stretching frequency of the free molecule averaged over the two rotational-vibration branches P and R of the gas-phase molecule is 4384 cm^{-1}. The comparison with the experimental frequency of 4161 cm^{-1} [35] shows the overestimation of the calculated value by 223 cm^{-1}. The discrepancy originates in the exchange-correlation functional and parameters of the MD simulation. Because the GGA functional[26] overestimates the bond strength of H_2, the frequency is higher than that experimentally observed.[35] The calculated frequency is weakly dependent on the simulation temperature, the simulation time, and the time step used in the MD simulation. E.g., a variation of temperature between 300 and 20 K leads to changes of the stretching frequency smaller than 10 cm^{-1}. Tuning of parameters of the simulation, i.e., the extension of the simulation time and the shortening of the time step, improves agreement between calculated frequencies and experimental data. To keep the cost of the simulation at a reasonable level, we performed all simulations at 20 K with a time step 1 fs and extended the simulation time to 4 ps. The frequencies reported in Table 4 are unscaled with full consideration of effects of anharmonic vibrations.

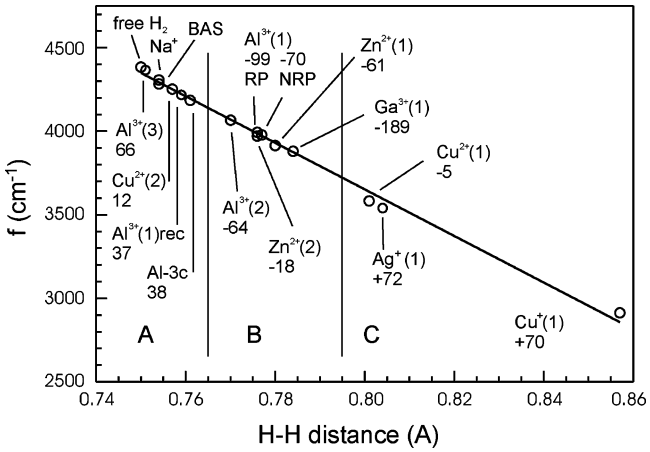

Figure 8. Stretching frequencies as a function of the bond length of the H_2 molecule adsorbed on different active sites. The number below the symbol of the cation is the dissociation energy indicating the capability of the site to dissociate the H_2 molecule. The full line is the least-squares fit. Vertical lines separate three groups of sites A, B, and C.

The stretching frequencies calculated for different active sites are directly comparable with the positions of bands in IR spectra. The spectrum of H−MOR consists of three bands centered at 4195, 4100, and 4028 cm^{-1}.[36] The broad band at the high-frequency side corresponds to a high-frequency satellite, i.e., to a combination mode of the H−H stretching with oscillations of H_2 adsorbed at BAS,[37] blue shifted by 34 cm^{-1} relative to the free molecule.[35] The bands at 4100 and 4028 cm^{-1} correspond to molecules physisorbed at BAS and chemisorbed at Lewis sites, respectively.[36]

The MD simulations provide stretching frequencies well correlated with the H−H interatomic distance of the adsorbed H_2 molecule (Figure 8). The calculated downshift for H_2 at BAS of 101 cm^{-1}, relative to the free molecule (cf. Table 4), is larger

than the shift 61 cm^{-1} observed by Kazansky.[36] The too large shift is due to the GGA approach. The PW91 functional[26] performs well for bonding within the zeolite framework but overestimates bonding within free and weakly adsorbed H_2. This leads to a H−H stretching frequency shifted to higher frequencies. Very small adsorption energy for H_2 on Al^{3+}(3) (cf. Table 3) indicates that the strength of intramolecular bonding is similar to that in the free molecule and the calculated frequency shift of +81 cm^{-1} is probably also overestimated. The adsorption on sites weaker than BAS, such as the Na^+ cation, produces a frequency between that for H_2 on BAS and for a free molecule. In mordenite, adsorption on such sites forms a shoulder at the high-frequency side of the band of H_2 at BAS; in ZSM-5 such states give rise to a band at $\Delta f = +20$ cm^{-1}.[36]

The band of H_2 adsorbed at Lewis sites ranging from ∼4100 to ∼3950 cm^{-1} is centered at 4028 cm^{-1}. Relative to H_2 on BAS the shifts range from 0 to −150 cm^{-1} with a maximum at −72 cm^{-1}. Our calculated shifts allow the assignment of these Lewis sites. They correspond to weak Lewis sites denoted in Figure 8 as group A. For zeolites not containing exchanged metal cations, this group of active sites consists mainly of reconstructed Al^{3+}(1) EFAl sites and of planar three-coordinated surface Al-3c sites.

For the adsorption on Zn^{2+}(2) and Zn^{2+}(1) sites, our calculated shifts relative to H_2 on BAS are −312 and −369 cm^{-1} (cf. Table 4). The stretching frequencies observed for H_2 adsorbed on Lewis sites in Zn-exchanged mordenite form a broad band with a maximum at $\Delta f \sim -73$ cm^{-1} and a shoulder extending to $\Delta f \sim -200$ cm^{-1}.[36] The band attributed to Lewis sites therefore does not correspond to molecular adsorption of H_2 on extraframework Zn^{2+} cations. As discussed in the following section, Zn^{2+} cations dissociate H_2 via a strongly exothermic process. The H_2 stretching band observed in the IR spectra is due to adsorption on weaker Lewis sites on which H_2 does not dissociate. Similarly, no bands are experimentally observed to downshift −220 to −300 cm^{-1} to be correlated with extraframework aluminum cations and a −600 to −700 cm^{-1} for molecular adsorption of H_2 on Ga^{3+}.

The adsorption of H_2 in Ag-exchanged zeolites was reported for A zeolite. Wang et al.[38] investigated reversible reduction−oxidation processes of Ag^+ with H_2 and O_2 and reported FTIR spectra for the interval 2800−4000 cm^{-1}. The frequency range corresponding to molecular adsorption of H_2 on BAS at ∼4100 cm^{-1} is not reported. The spectra are not well resolved, displaying a broad band of the hydrogen-bonded O−H stretching modes ranging from 3700 to 3400 cm^{-1}. Upon adsorption of H_2, a distinct band at 3619 cm^{-1} appears, providing evidence of the dissociation $H_2 \rightarrow H^+ + H^-$ and formation of Brønsted acid sites. At the same time a weak band appears at ∼3300 cm^{-1}, not assigned to any specific kind of the adsorption. Compared with the stretching of H_2 adsorbed on the BAS of ∼4100 cm^{-1},[39] this band is downshifted by ∼800 cm^{-1}. Our calculated stretching frequency of H_2 adsorbed on Ag^+ is downshifted by 744 cm^{-1}. Hence the band observed at ∼3300 cm^{-1} corresponds to the nondissociative adsorption of H_2 on a single Ag^+ cation. In contrast to the exothermic dissociation of H_2 on Zn^{2+}, dissociation of H_2 on Ag^+ is a strongly endothermic process (cf. Table 3 and the following section).

A huge downshift of the H_2 stretching frequencies of 1370 cm^{-1} is calculated for H_2 adsorbed on the Cu^+ cation (cf. Table 4 and Figure 8). Experimental data reported recently for Cu-exchanged ZSM-5[39] and CHA[42] confirm the existence of a dramatic low-frequency shift of the H_2 stretching on Cu−Z species. For H_2 adsorption on a Cu^+ cation in ZSM-5, Serykh and Kazansky[39] observed an unusually high adsorption energy and stretching bands downshifted by 805, 980, and 1030 cm^{-1} relative to the well distinguished band corresponding to adsorption on BAS. The bands are assigned to adsorption on Cu species located in different sites in the MFI structure. The largest shift observed for the H_2-stretching mode of −1030 cm^{-1}, however, is by 340 cm^{-1} smaller than our calculated shift of −1370 cm^{-1}. This discrepancy is due to the GGA approximation. Although GGA performs well for bonding within the zeolite framework, it overestimates the strength of the Cu−H bond. Too strong bonding to the transition metal induces a too large activation of the adsorbed molecule, leading to an overestimation of the downshift of the H_2-stretching mode. A similar effect of slightly incorrect distribution of the electron density calculated by GGA functionals is observed for bonding of CO on Cu^+ in the MFI framework. An exaggerated back-donation via d_π-orbitals leads to overfilling of antibonding states in CO. Because of the exaggerated weakening of the C−O bond, the calculated stretching frequency is downshifted in contrast to the observed upshift. Nachtigall et al. developed a rescaling procedure that brings the calculated frequencies to "near spectroscopic accuracy".[40] The rescaling was demonstrated to work also for CO adsorption in other zeolite structures, e.g., FER.[41] Recently Ugliengo et al. investigated adsorption of H_2 on Cu-exchanged chabazite.[42] Using the BLYP functional and a basis set adopted for Cu, they calculate for the adsorbed H_2 an interatomic distance of 0.82 Å. Their calculated downshift of $\Delta f \sim -1100$ cm^{-1} compares well with the experimental value −1030 cm^{-1}. The PW91 functional used in the present work provides the H−H distance 0.86 Å and a too large downshift of 1370 cm^{-1}.

In the complex Z−Cu−H_2 a quasi-planar coordination of the transition metal is formed. On one side Cu binds to two O atoms of the framework and on the other side two H atoms complete the planar coordination of the transition metal. In CHA Ugliengo et al.[42] observed quasi-planar complexes similar to those formed in MOR. The formation of a quasi-planar Z−Cu−H_2 complex therefore seems to be independent of the zeolite structure and characteristic for the adsorption of H_2 in Cu-exchanged zeolites.

Heating of Cu−ZSM-5 in oxygen at 873 K leads to almost complete disappearance of all low-frequency bands assigned to H_2-stretching modes at 3075, 3125, and ∼3300 cm^{-1}. At the same time a new band at $\Delta f \sim -35$ cm^{-1} relative to the band of H_2 adsorbed at BAS appears.[39] The disappearance of low-frequency bands means that Cu^+ cations are no longer available for the adsorption of H_2. During the thermal treatment in O_2, oxidation of extraframework Cu^+ cations occurs and two types of active sites are expected to appear: Cu^{2+}(1) and Cu^{2+}(2). The former represents the Cu^{2+} cation deposited on the inner surface of the zeolite and making a contact to just one framework Al site. In the latter two contacts to zeolite Al sites are established. Because of the low concentration of the framework Al sites (Si/Al = 25), formation of Cu^{2+}(1) appears to be more probable. A H_2 stretching band shifted by ca. −700 cm^{-1} (cf. Table 4) calculated for Cu^{2+}(1) sites with a single Cu^{2+} cation deposited in the extraframework position, however, is not observed in the IR spectra. The new band at −35 cm^{-1} compares to a weak adsorption center similar to Cu^{2+}(2) for which the calculated stretching frequency of is downshifted by 31 cm^{-1} (cf. Table 4). We therefore agree with the interpretation of Kazansky that calcination in O_2 produces some oxo-species.[39] Due to bonding with O atoms, Cu^{2+} in such oxo-complexes represents only a weak adsorption site similar to Cu^{2+}(2). Both phenomena—the disappearance of the low-frequency bands and a formation of the band at −35 cm^{-1}—show that upon

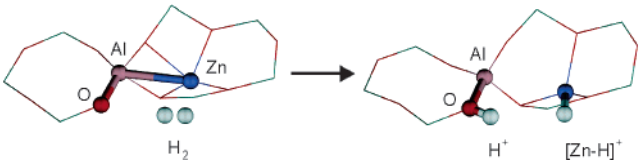

Figure 9. Dissociation of H_2 on the configuration in Zn−MOR representing a reaction pathway. The configuration is formed by a Al/Si substitution in the T4 site shared by the 4MR and the 5MR and a Zn^{2+} cation bound in the 5MR. The left panel shows the adsorbed neutral molecule and the right panel the dissociation products. A Brønsted acid site forms on the oxygen atom bound to the Al site in the 4MR and the $[Zn-H]^+$ cation resides on the 5MR.

calcination in O_2 a conversion of extraframework Cu^+ cations into weak adsorption centers, similar to weak Cu^{2+}(2) Lewis sites, takes place. Heating in CO restores the original spectrum.[39] This means that CO destroys Cu^{2+} oxo-complexes producing again monovalent single Cu^+ cations in extraframework positions.

3.2. Dissociative Adsorption. Reaction Pathway. Depending on the character of the active site, adsorption of hydrogen can lead either to the formation of a molecular adduct or to the dissociation of the H_2 molecule according to

$$H_2 \rightarrow H^- + H^+ \quad (1)$$

Both products of the dissociation, the proton H^+ and the hydrogen anion H^-, are stabilized by interaction with the zeolite framework or with the extraframework cation. The negatively charged framework oxygen atoms attract the proton. Formation of a hydroxyl group restores a Brønsted acid site. The hydride anion is repulsed by the framework and attracted to an extraframework cation forming a $[M - H]^+$ metal hydride cation according to

$$MOR^{2-} - M^{2+} + H_2 \rightarrow H - MOR^- - [M - H]^+ \quad (2)$$

In Zn−ZSM-5 the continuous formation of Brønsted acid sites leads to an increasing intensity of the O−H stretching band at 3610 cm^{-1}. The formation of the $Zn-H^+$ ion is detected by the growing intensity of the Zn−H stretching band at 1934 cm^{-1}.[36]

A local configuration in a zeolite with a high capacity to locally stabilize H^+ and H^- represents a reaction pathway for the dissociation of H_2. In our recent paper on Zn−MOR an analysis of reaction pathways in Zn-exchanged mordenite is reported.[14] A configuration of the most efficient reaction pathway is displayed in Figure 9. This configuration contains a Al/Si substitution in the energetically relatively unfavorable T4 site shared by the 5MR and 4MR of the framework. Such a location of Al makes the configuration more active and the T4 site shared by two rings is advantageous for the separation of the reaction products. The proton is attached to an O atom of the 4MR and the H^- anion binds to the extraframework cation located on the 5MR (Figure 9). Because of the high reactivity, the configuration of the reaction pathway displayed in Figure 9 easily dissociates H_2 and is able to break the C−H bond of the saturated hydrocarbon.[14]

Energetics. The dissociation energies of active sites are listed in Table 3 and displayed in Figure 8. The extraframework cations are located in the configuration representing the reaction pathway, displayed in Figures 3a and 9, except for the NRP configuration (Figure 3b). The calculated dissociation energies span a huge interval from −190 to 72 kJ/mol. The relation between the dissociation energies and the degree of activation of the H_2 molecule indicates again three different categories of active sites denoted in Figures 5−8 as A, B, and C.

Group A comprises weak sites causing only a slight activation of the H−H bond; they are unable to dissociate the H_2 molecule. To this group belong the three-coordinated Al site forming a framework defect, the Brønsted acid site, and the extraframework Na^+ cation. All these sites exhibit low adsorption energies (cf. Table 3 and Figure 6) and a low degree of H−H bond activation (Figure 7). The calculated dissociation energies are strongly endothermic and show that on such sites the dissociation of H_2 is disfavored because they are not able to stabilize dissociation products. Note that also "strong" cations, such as Cu^{2+} and Al^{3+}, belong to this group. These cations, however, are not in typical extraframework positions but integrated within the zeolite framework. The change from an extraframework position to an interstitial framework site leads to a considerable decrease of the adsorption strength of such cations and converts them to weak nonreactive adsorption sites.

Group B consists of multivalent extraframework cations that cause intermediate activation of the H−H bond and strongly favor dissociation. Typical representatives are Zn^{2+}, Al^3, and Ga^{3+}. In adsorbed molecular hydrogen the H−H bond elongation ranges from 0.02 to 0.035 Å (Figure 8). These metals form stable hydrides. In the zeolite, cationic hydrides are formed. The cations $[Zn-H]^+$, $[Al-H]^{2+}$, and $[Ga-H]^{2+}$ compensate the negative charge of the zeolite framework and represent locally stable reaction products of H_2 dissociation. More exothermic dissociation energies are observed for trivalent than for bivalent cations, −189, −99, and −61 kJ/mol for Ga^{3+}, Al^{3+}, and Zn^{2+}, respectively. The much more exothermic dissociation energy for Ga^{3+} compared with Al^{3+} is due to the smaller ionic radius and higher electronegativity of the former. Note that the dissociative power of an extraframework cation strongly depends on the location of the framework Al site. For two configurations with Al^{3+} on the 5MR, displayed in Figure 3 and denoted as a reaction pathway and nonreaction pathway (RP, NRP), the same degree of activation of the H_2 molecule is observed (Figures 5−8). The dissociative power of the Lewis site, however, increases by 29 kJ/mol for the cation in the configuration representing a reaction pathway (Table 3 and Figure 8). This results from the much better stabilization of the proton by local configuration of the reaction pathway.

Group C is formed by the monovalent extraframework cations Cu^+ and Ag^+ causing an extremely strong activation of the H−H bond. A reason behind the high degree of activation is the rather loose interaction of the cation with the framework. The distance r_1 between Cu^+ and Ag^+ and the closest framework oxygens is much larger than that for cations in group B (cf. Table 3 and Figure 8). The loose contact is caused by the low valency and high electronegativity of the metal ion. Because of the high electronegativity, the positive charge of the cation is smaller than that of atoms in group B with lower electronegativities resulting in lower interaction energy between the cation and the framework. The lower degree of stabilization of the Cu^+ and Ag^+ cations in extraframework sites leads to a strong molecular adsorption as evidenced by short distances between the cation and the adsorbed molecule (Figure 5) and high adsorption energies (Figure 6).

Despite the strong activation of the adsorbed molecule single Cu^+ and Ag^+ cations cannot dissociate the H_2 molecule as indicated by strongly endothermic dissociation energies of +70 and +72 kJ/mol (Table 3 and Figure 8). The dissociation produces a proton and a neutral hydride M−H (M = Cu, Ag) molecule. The proton binds to an O site of the framework

forming a Brønsted acid site on which the neutral M−H molecule is adsorbed. The acid form of the zeolite, however, is considerably less stable than the ion-exchanged structure. E.g., the H form of gmelinite is by ∼190 kJ/mol less stable than the Na-exchanged structure.[43] Moreover, the adsorption energies of neutral molecules are lower for acid zeolites than for cation-exchanged zeolites. Because the dissociation products are considerably less stable than adsorbed molecular hydrogen, a single Cu^+ cation deposited in a zeolite cannot act as an active center for the dissociation of H_2. In agreement with this conclusion a series of H−H stretching frequencies assigned to long-lived H_2 molecules adsorbed on the Cu^+ cation is observed.[39]

An increased ability to dissociate H_2 is observed for the Cu^{2+} cation. Figure 8 shows that the activation of the H−H bond on $Cu^{2+}(1)$ is comparable with that of the Ag^+ cation and the dissociation energy is −5 kJ/mol (Table 3 and Figure 8). The capacity to dissociate H_2, however, is observed for the cation connected to one Al site of the zeolite framework only. As already discussed above, oxidation of Cu^+ to Cu^{2+} in O_2 produces oxo-species. The Cu^{2+} cation integrated in such an oxo-complex exhibits only weak adsorption power similar to $Cu^{2+}(2)$ and is unable to dissociate H_2.[39]

Any stabilization of the extraframework cation causes a decrease of the adsorption strength and of the dissociative power of the Lewis site. The stability of an extraframework cation increases with the number of contacts formed between the cation and AlO_4 tetrahedra in the framework. For Al−MOR configurations with the Al^{3+} cation in the extraframework position with one to three contacts to framework AlO_4 tetrahedra (sites $Al^{3+}(1)$, $Al^{3+}(2)$ and $Al^{3+}(3)$), the dissociation energies are −99, −64, and +66 kJ/mol, respectively. A similar trend is observed for extraframework cations Zn^{2+} and Cu^{2+}. Upon replacement of $Zn^{2+}(1)$ by $Zn^{2+}(2)$ the dissociation energy decreases from −61 to −18 kJ/mol, and for $Cu^{2+}(1) \rightarrow Cu^{2+}(2)$ from −5 to +12 kJ/mol. When an extraframework cation is placed in such a position on the inner zeolite surface where the number of contacts between the cation and the framework Al sites equals its valency, the cation forms strong bonds to the framework and is nearly fully integrated into the zeolite framework. The integrated cation is located deep in the framework far away from the inner surface. For this reason molecules cannot approach the cation, and since furthermore bonding between O atoms of the framework and such a cation is saturated, the adsorption capacity is weak. The local reconstruction induced by the stabilization of the extraframework cation changes the bonding character of the site and converts the configuration into a weak nonreactive Lewis site. Among stabilized extraframework cations the largest loss of dissociative power is observed for $Al^{3+}(3)$ and $Cu^{2+}(2)$ sites (dissociation energies +66 and +12 kJ/mol, respectively). Because of a small ionic radius,[34] both of these cations penetrate the framework and reside in interstitial sites between the framework Al atoms.

4. Conclusions

Our comparison of adsorption properties of active sites in mordenite includes the Brønsted acid site, a three-coordinated surface Al site, an extraframework Al site, and bare extraframework cations located in the five-membered ring of the zeolite. This location does not correspond with the experimental position of the hydrated cation observed in the six-membered ring. In dehydrated mordenite, however, the bare cation adsorbed on the five-membered ring represents one of the locally stable structures. Such a cation exhibits considerable activity and is well accessible from the main channel of the zeolite. The simulation of the molecular and dissociative adsorption of H_2 in mordenite indicates the existence of three different groups of active sites:

(i) Weak sites, exhibiting small activation power, unable to dissociate H_2. This group comprises the Brønsted acid site, weak Lewis sites (Na^+), dehydrated surface sites (tree-coordinated Al), and extraframework cations integrated into interstitial positions of the framework ($Al^{3+}(3)$, $Cu^{2+}(2)$).

(ii) Lewis sites with intermediate activation power supporting the dissociation $H_2 \rightarrow H^{++} H^-$. The dissociation is enabled by the stabilization of the H^- anion via bonding to the extraframework cation and by binding of the H^+ cation to O atoms of the framework. This group of Lewis sites includes the polyvalent $Zn^{2+}(2)$, $Zn^{2+}(1)$, $Al^{3+}(2)$, $Al^{3+}(1)$, and $Ga^{3+}(1)$ cations. Local configurations in a zeolite with an extraframework cation exhibiting exothermic dissociation energies represent reaction pathways for dissociation of H_2.

(iii) Monovalent cationic Lewis sites Cu^+ and Ag^+ inducing a strong activation of H_2, but not supporting dissociation of H_2. These extraframework cations exhibit large adsorption energies 60−90 kJ/mol. The dissociation of H_2, however, is endothermic producing an energetically disadvantaged neutral hydride molecule.

Adsorption and reaction properties of a cation in extraframework positions of a zeolite depend not only on characteristics of the cation itself, i.e., ionic charge, ionic radius, and electronegativity, but also on the bonding between the cation and the framework. Bulky alkali metal cations with low electronegativity are weakly bound to the framework and are weak sites for adsorption of molecules. Polyvalent cations with intermediate electronegativity are via strong bonding to the zeolite framework converted into weak adsorption centers. A strong interaction with the zeolite framework leads to saturation of their bonding capacity, thus diminishing the adsorption strength and reactivity of the cation. For this reason very weak adsorption energies and low activation of the H_2 molecule are observed for $Al^{3+}(3)$ and $Cu^{2+}(2)$ cations integrated into interstitial framework positions.

Polyvalent cations with intermediate electronegativity such as Zn^{2+}, Al^{3+}, and Ga^{3+} deposited on a rigid part of the framework, like the five-membered ring, represent reaction centers with high adsorption energies. The relatively low electronegativity of Zn, Al, and Ga atoms allows a transfer of electron density from metal to the H atom, leading to the formation of metal hydrides.[34] The cations of these atoms placed in extraframework sites of a zeolite can also bind the H^- anion forming a $[M-H]^{n+}$ hydride. Such cationic hydrides are stabilized in the extraframework position and represent reaction products. Zeolites with bare Zn^{2+}, Al^{3+}, and Ga^{3+} cations in extraframework sites therefore act as effective catalysts of the intrazeolite dissociation of H_2.

Monovalent Cu^+ and Ag^+ cations with relatively low electronegativity are only loosely bound to the zeolite framework and therefore represent strong centers for molecular adsorption. The molecules are attracted to such cations at a short distance and activated to a high extent. Single monovalent Cu^+ and Ag^+ cations, however, cannot dissociate the H_2 molecule because they cannot stabilize the dissociation products.

Acknowledgment. This work has been supported by the Austrian Science Funds under Project No. P17020-PHYS and by the Institut Français du Pétrole. Computational resources were

partly granted by the Computing Center of Vienna University (Schrödinger Cluster).

References and Notes

(1) Dyer, A. In *Encyclopedia of Inorganic Chemistry*; King, R. G., Ed.; John Wiley and Son: New York, 1994; Vol. 8, p 4363.
(2) Benco, L.; Bucko, T.; Hafner, J.; Toulhoat, H. *J. Phys. Chem. B* **2004**, *108*, 13656.
(3) Jentoft, F. C.; Gates, B. C. *Top. Catal.* **1997**, *4*, 1.
(4) Haag. W. O.; Dessau, R. M. *Proceedings of the 8th International Congress on Catalysis*; Verlag Chemie: Weinheim, 1984; Vol. 2, p 305.
(5) Cairon, O.; Chevreau, T.; Lavalley, J.-C. *J. Chem. Soc., Faraday Trans.* **1998**, *94*, 3090.
(6) Seff, K. *Micropor. Mesopor. Mater.* **2005**, *85*, 351.
(7) Seff, K. *J. Phys. Chem. B* **2005**, *109*, 13840.
(8) Jiao, J.; Altwasser, S.; Wang, W.; Weitkamp, J.; Hunger, M. *J. Phys. Chem. B* **2004**, *108*, 14305.
(9) Gola, A.; Rebours, B.; Milazzo, E.; Lynch, J.; Benazzi, E.; Lacombe, S.; Delevoye, L.; Fernandez, C. *Micropor. Mesopor. Mater.* **2000**, *40*, 73.
(10) Omegna, A.; van Bokhoven, J. A.; Prins, R. *J. Phys. Chem. B* **2003**, *107*, 8854.
(11) Omegna, A.; Haouas, M.; Kogelbauer, A.; Prins, R. *Micropor. Mesopor. Mater.* **2001**, *46*, 177.
(12) Arribas, M. A.; Martinez, A. *Appl. Catal., A* **2002**, *230*, 203.
(13) Benco, L.; Demuth, T.; Hafner, J.; Hutschka, F.; Toulhoat, H. *J. Catal.* **2002**, *209*, 480.
(14) Benco, L.; Bucko, T.; Hafner, J.; Toulhoat, H. *J. Phys. Chem. B* **2005**, *109*, 20361.
(15) Mortier, W. J. *Compilation of Extraframework Sites in Zeolites*; Butterworth: London, 1982.
(16) Demuth, T.; Hafner, J.; Benco, L.; Toulhoat, H. *J. Phys. Chem. B* **2000**, *104*, 4593.
(17) Bucko, T.; Benco, L.; Hafner, J. *J. Phys. Chem. B* **2005**, *109*, 7345.
(18) Bhering, D. L.; Ramirez-Solis, A.; Mota, J. J. A. *J. Phys. Chem. B* **2003**, *107*, 4342.
(19) Bucko, T.; Benco, L.; Hafner, J. *J. Chem. Phys.* **2003**, *118*, 8437.
(20) Bugaev, L. A.; van Bokhoven, J. A.; Sokolenko, A. P.; Latokha, Y. V.; Avakyan, L. A. *J. Phys. Chem. B* **2005**, *109*, 10771.
(21) Kresse, G.; Hafner, J. *J. Phys. Chem. B* **1993**, *48*, 13115.
(22) Kresse, G.; Hafner, J. *J. Phys. Chem. B* **1994**, *49*, 14251.
(23) Kresse, G.; Furthmüller, J. *Comput. Mater. Sci.* **1996**, *6*, 15.
(24) Kresse, G.; Furthmüller, J. *Phys. Rev. B* **1996**, *54*, 11169.
(25) Perdew, J. P.; Zunger, A. *Phys. Rev. B* **1981**, *23*, 5048.
(26) Perdew, J. P.; Chevary, A.; Vosko, S. H.; Jackson, K. A.; Pedersen, M. R.; Singh, D. J.; Fiolhais, C. *Phys. Rev. B* **1992**, *46*, 6671.
(27) Vanderbilt, D. *Phys. Rev. B* **1990**, *41*, 7892.
(28) Kresse, G.; Hafner, J. *J. Phys.: Condens. Matter* **1994**, *6*, 8245.
(29) Blochl, P. E. *Phys. Rev. B* **1994**, *50*, 17953.
(30) Kresse, G.; Joubert, D. *Phys. Rev. B* **1999**, *59*, 1758.
(31) Jeanvoine, Y.; Angyan, J.; Kresse, G.; Hafner, J. *J. Phys. Chem. B* **1998**, *102*, 5573.
(32) Nose, S. *J. Chem. Phys.* **1984**, *81*, 511.
(33) Allen, M. P., Tildesley, D. J., *Computer Simulations of Liquids*; Clarendon: Oxford, 1987.
(34) www.webelements.com
(35) Stoicheff, B. P. *Can. J. Phys.* **1957**, *35*, 730.
(36) Kazansky, V. B. *J. Catal.* **2003**, *216*, 192.
(37) Kazansky, V. B. *J. Mol. Catal. A: Chem.* **1999**, *141*, 83.
(38) Wang, P.; Yang, S.; Kondo, J. K.; Domen, K.; Baba, T. *Bull. Chem. Soc. Jpn.* **2004**, *77*, 1627.
(39) Serykh, A. I.; Kazansky, V. B. *Phys. Chem. Chem. Phys.* **2004**, *6*, 5250.
(40) Bludsky, O.; Silhan, M.; Nachtigalova, D.; Nachtigal, P. *J. Phys. Chem. A* **2003**, *107*, 10381.
(41) Bludsky, O.; Silhan, M.; Nachtigall, P.; Bucko, T.; Benco, L.; Hafner. *J. Phys. Chem. B* **2005**, *109*, 9631.
(42) Solans-Monfort, X.; Branchadell, V.; Sodupe, M.; Zicovich-Wilson, C. M.; Gribov, E.; Spoto, G.; Busco, C.; Ugliengo, P. *J. Phys. Chem. B* **2004**, *108*, 8278.
(43) Benco, L.; Demuth, T.; Hafner, J.; Hutschka, F. *Micropor. Mesopor. Mater.* **2001**, *42*, 1.